FLOW OF AN ERYING-POWELL FLUID OVER A STRETCHING SHEET IN PRESENCE OF CHEMICAL REACTION

by

Ilyas KHAN[a]*, Muhammad QASIM[b], and Sharidan SHAFIE[a]

[a] Basic Engineering Sciences Department, College of Engineering, Majmaah University, Majmaah, Saudi Arabia
[b] Department of Mathematics, COMSATS Institute of Information Technology, Islamabad, Pakistan

Original scientific paper
DOI: 10.2298/TSCI131129111K

In this paper we study the flow of an incompressible Erying-Powell fluid bounded by a linear stretching surface. The mass transfer analysis in the presence of destructive/generative chemical reactions is also analyzed. A similarity transformation is used to transform the governing partial differential equations into ordinary differential equations. Computations for dimensionless velocity and concentration fields are performed by an efficient approach namely the homotopy analysis method and numerical solution is obtained by shooting technique along with Runge-Kutta-Fehlberg integration scheme. Graphical results are prepared to illustrate the details of flow and mass transfer characteristics and their dependence upon the physical parameters. The values for gradient of mass transfer are also evaluated and analyzed. A comparison of the present solutions with published results in the literature is performed and the results are found to be in excellent agreement.

Key words: *mass transfer, destructive/generative chemical reactions, Erying-Powell fluid, analytical solution, numerical solution*

Introduction

The flows of non-Newtonian fluids have been of great importance and increasing interest for the last few decades. Perhaps, it is due to their several engineering and technological applications. Few examples of the non-Newtonian fluids are coal water, jellies, toothpaste, ketchup, food products, inks, glues, soaps, blood, and polymer solutions. It is well known that there is no unique relationship available in the literature like Newtonian law of viscosity for viscous fluids that can describe the rheology of all the non-Newtonian fluids. It is due the diversity of non-Newtonian fluids in nature in terms of their viscous and elastic properties. Mathematical systems for non-Newtonian fluids are of higher order and complicated in comparison to the Newtonian fluids. Despite of all these difficulties and complexities, several researchers in the field are involved in making valuable contributions to the studies of non-Newtonian fluid dynamics [1-10]. The non-Newtonian fluid models vary in their complexity and ability to capture different physical phenomena. Of course, no single model can capture all the features of the non-Newtonian fluids complexities and hence different models are used to represent different characteristics of the non-Newtonian fluids. Among these fluid models the Powell-Erying flu-

* Corresponding author; e-mail: ilyaskhanqau@yahoo.com; i.said@mu.edu.sa
Former affiliation: Department of Mathematical Sciences, Faculty of Science, University of Technology Malaysia, Skudai, Malaysia

id model [11-13] is important as it can be deduced from a kinetic theory of gases rather than the empirical relation as in the power law model. Also it correctly reduces to Newtonian behaviour for low and high shear rates for otherwise pseudoplastic systems, whereas the power law model indicates an infinite effective viscosity for low shear rate, thus limiting its range of applicability. Furthermore, this fluid model appears to be quite accurate and consistent in calculation of fluid time scale at various polymer concentrations [14, 15].

On the other hand, the interest of researchers in stretching flows with boundary layer approximation has now increased substantially in recent years in view of its significant applications in the polymer industry and manufacturing processes including wire drawing, spinning of filaments, hot rolling, crystal growing, fiber production, paper production, wire drawing, drawing of plastic films, metal and polymer extrusion, and metal spinning. Crane [16] in his pioneering work introduced the concept of stretching flow and obtained a closed form solution for the steady flow of viscous fluid due to a linearly stretching sheet. The transport of mass and momentum of chemical reactive species in the flow caused by a linear stretching sheet is discussed by Andersson *et al.* [17]. Takhar *et al.* [18] investigated the (MHD) flow and mass transfer in a viscous fluid over a stretching surface. Akyildiz *et al*. [19] studied the same flow problem for second grade fluid filling a porous medium. Hayat *et al.* [20] studied the MHD flow and mass transfer in a Maxwell fluid past a porous shrinking sheet in the presence of destructive/generative chemical reaction. Motivated by the previous investigations, the present study aims to investigate the stretching flow of non-Newtonian Erying-Powell fluid in the presence of chemical reactive species. The flow is due to a linear stretching surface. Numerical solution is obtained by shooting technique along with Runge-Kutta-Fehlberg integration scheme and homotopy analysis method (HAM) [21-26] has been used in the development of series solutions. Convergence of series solutions is established and interesting observations are extracted through graphs and tables.

Problem formulation

Let us consider the steady 2-D flow of an incompressible Erying-Powell fluid in the half space $y > 0$. In addition the mass transfer effects are considered. The velocity $U_w(x)$ and the concentration $C_w(x)$ of the stretching sheet is proportional to the distance x from origin O, where $C_w(x) > C_\infty$ (see fig. 1).

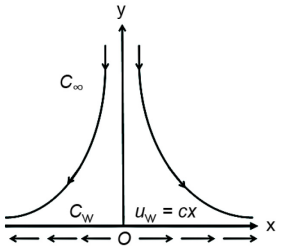

Figure 1. Physical model and co-ordinate system

The boundary layer flow is governed by the following equations [12, 17-19]:

$$\frac{\partial u}{\partial x}+\frac{\partial v}{\partial y}=0 \tag{1}$$

$$u\frac{\partial u}{\partial x}+v\frac{\partial u}{\partial y}=\left(\nu+\frac{1}{\rho\tilde{\beta}C^*}\right)\frac{\partial^2 u}{\partial y^2}-\frac{1}{2\rho\tilde{\beta}C^{*3}}\left(\frac{\partial u}{\partial y}\right)^2\frac{\partial^2 u}{\partial y^2} \tag{2}$$

$$u\frac{\partial C}{\partial x}+v\frac{\partial C}{\partial y}=D\frac{\partial^2 C}{\partial y^2}-k_1 C \tag{3}$$

where $\tilde{\beta}$ and C^* are the characteristics of Powell-Erying model, u, v – the velocity components along x- and y-axes, ρ – the fluid density, ν – the kinematic viscosity, D – the mass diffusion, C – the concentration field, and k_1 – the reaction rate.

The corresponding boundary conditions are:

$$U = U_{\mathrm{w}}(x) = cx, \qquad v = 0, \qquad C = C_{\mathrm{w}}(x) = C_{\infty} + bx \qquad \text{at} \qquad y = 0 \tag{4}$$

$$u = 0, \qquad C = C_{\infty} \qquad \text{as} \qquad y \to \infty \tag{5}$$

where c is the stretching rate and the subscripts w and ∞ are written for the wall and free stream conditions.

Introducing the following similarity transformations:

$$\eta = \sqrt{\frac{c}{\nu}}y, \qquad u = cxf'(\eta), \qquad v = -\sqrt{c\nu}f(\eta), \qquad \varphi = \frac{C - C_{\infty}}{C_{\mathrm{w}} - C_{\infty}} \tag{6}$$

into eqs. (1)-(4), the continuity equation is identically satisfied and eqs. (2)-(5) become:

$$(1+K)f''' - f'^2 + ff'' - K\Gamma f''^2 f''' = 0 \tag{7}$$

$$\varphi'' + \mathrm{Sc}(f\varphi' - \varphi f' - \gamma\varphi) = 0 \tag{8}$$

$$f = 0, \qquad f' = 1, \qquad \varphi = 1 \qquad \text{at} \qquad \eta = 0$$
$$f' = 0, \qquad \varphi = 0 \qquad \text{at} \qquad \eta \to \infty \tag{9}$$

where

$$\mathrm{Sc} = \frac{\nu}{D}, \qquad K = \frac{1}{\mu\tilde{\beta}C^*}, \qquad \Gamma = \frac{x^2c^3}{2\nu C^{*2}}, \qquad \gamma = \frac{k_1}{c} \tag{10}$$

Furthermore, Sc, K, and γ are the Schmidt number, Deborah, and chemical reaction parameters, respectively, and μ is the viscosity coefficient. The local skin friction coefficient and Sherwood number (surface mass transfer) on the surface are:

$$C_{fx} = \frac{\tau_{xy}\big|_{y=0}}{\rho u_{\mathrm{w}}^2}, \qquad \mathrm{Sh} = \frac{-xD\left(\dfrac{\partial C}{\partial y}\right)_{y=0}}{C_{\mathrm{w}} - C_{\infty}} \tag{11}$$

In dimensionless form eq. (11) can be written:

$$\mathrm{Re}_x^{1/2}\, C_{fx} = \left\{(1+K)f''(0) - \frac{K\Gamma}{3}f'''(0)\right\}, \qquad \mathrm{Sh}\,\mathrm{Re}_x^{-1/2} = -\varphi'(0) \tag{12}$$

Solution methodologies

Homotopy analysis method

In order to derive the HAM solutions, we chose the base functions of the form:

$$\{\eta^k \exp(-n\eta), \qquad k \geq 0, \qquad n \geq 0\} \tag{13}$$

and

$$f(\eta) = a_{0,0}^0 + \sum_{n=0}^{\infty}\sum_{k=0}^{\infty} a_{m,n}^k \eta^k \exp(-n\eta), \qquad \varphi(\eta) = \sum_{n=0}^{\infty}\sum_{k=0}^{\infty} b_{m,n}^k \eta^k \exp(-n\eta) \tag{14}$$

where $a_{m,n}^k$ and $b_{m,n}^k$ are the coefficients. The initial approximations are f_0 and φ_0 and auxiliary linear operators are:

$$f_0(\eta) = 1 - \exp(-\eta), \qquad \varphi_0(\eta) = \exp(-\eta) \tag{15}$$

$$\mathbf{L}_f(f) = \frac{\mathrm{d}^3 f}{\mathrm{d}\eta^3} - \frac{\mathrm{d}f}{\mathrm{d}\eta} \tag{16}$$

$$\mathbf{L}_\varphi(f) = \frac{\mathrm{d}^2 f}{\mathrm{d}\eta^2} - f \tag{17}$$

whence

$$\mathbf{L}_f[C_1 + C_2 \exp(\eta) + C_3 \exp(-\eta)] = 0 \tag{18}$$

$$\mathbf{L}_\varphi[C_4 \exp(\eta) + C_5 \exp(-\eta)] = 0 \tag{19}$$

and C_i (i = 1-5) are the arbitrary constants. The embedding parameter $p \in [0, 1]$, h_f and h_φ are non-zero auxiliary parameters. The problems at the 0$^{\text{th}}$ order are written:

$$(1-p)\mathbf{L}_f[f(\eta;\, p) - f_0(\eta)] = p h_f N_f[f(\eta;\, p)] \tag{20}$$

$$(1-p)\mathbf{L}_\varphi[\varphi(\eta;\, p) - \varphi_0(\eta)] = p h_\varphi N_\varphi[\varphi(\eta;\, p), \quad f(\eta;\, p)] \tag{21}$$

$$f(\eta;\, p)\big|_{\eta=0} = 0, \quad \left.\frac{\partial f(\eta;\, p)}{\partial \eta}\right|_{\eta=0} = 1, \qquad \left.\frac{\partial f(\eta;\, p)}{\partial \eta}\right|_{\eta=\infty} = 0 \tag{22}$$

$$\varphi(\eta;\, p)\big|_{\eta=0} = 1, \qquad \varphi(\eta;\, p)\big|_{\eta=\infty} = 0 \tag{23}$$

$$\mathbf{N}_f[\hat{f}(\eta,\, p)] = (1+K)\frac{\partial^3 \hat{f}(\eta,\, p)}{\partial \eta^3} + \hat{f}(\eta,\, p)\frac{\partial^2 \hat{f}(\eta,\, p)}{\partial \eta^2} - \left[\frac{\partial \hat{f}(\eta,\, p)}{\partial \eta}\right]^2 - K\Gamma\left[\frac{\partial^2 \hat{f}(\eta,\, p)}{\partial \eta^2}\right]^2 \frac{\partial^3 \hat{f}(\eta,\, p)}{\partial \eta^3} \tag{24}$$

$$N_\varphi[\varphi(\eta;\, p), \quad f(\eta;\, p)] = \frac{\partial^2 \varphi(\eta;\, p)}{\partial \eta^2} + \mathrm{Sc}\left[f(\eta;\, p)\frac{\partial \varphi(\eta;\, p)}{\partial \eta} - \varphi(\eta;\, p)\frac{\partial f(\eta;\, p)}{\partial \eta} - \gamma\varphi(\eta;\, p)\right] \tag{25}$$

The mentioned 0$^{\text{th}}$-order deformation eqs. (20) and (21) for $p = 0$ and $p = 1$ have the following solutions:

$$f(\eta;\, 0) = f_0(\eta), \qquad f(\eta;\, 1) = f(\eta) \tag{26}$$

$$\varphi(\eta;\, 0) = \varphi_0(\eta), \qquad \varphi(\eta;\, 1) = \varphi(\eta) \tag{27}$$

Obviously, when p increases from 0 to 1, $f(\eta, p)$ varies from initial guess $f_0(\eta)$ to the exact solution $f(\eta)$. Therefore, by Taylors' theorem and using eqs. (26) and (27), we get:

$$f(\eta;\, p) = f_0(\eta) + \sum_{m=0}^{\infty} f_m(\eta) p^m \tag{28}$$

$$\varphi(\eta;\, p) = \varphi_0(\eta) + \sum_{m=0}^{\infty} \varphi_m(\eta) p^m \tag{29}$$

$$f_m(\eta) = \frac{1}{m!} \frac{\partial^m f(\eta;\, p)}{\partial \eta^m}\bigg|_{p=0}, \qquad \varphi_m(\eta) = \frac{1}{m!} \frac{\partial^m \varphi(\eta;\, p)}{\partial \eta^m}\bigg|_{p=0} \tag{30}$$

Clearly, eqs. (20) and (21) involve non-zero auxiliary parameters h_f and h_φ. The convergence of the series (28) and (29) depends upon h_f and h_φ. The values of h_f and h_φ are selected such that the eqs. (28) and (29) are convergent at $p = 1$. Hence we write:

$$f(\eta) = f_0(\eta) + \sum_{m=0}^{\infty} f_m(\eta) \tag{31}$$

$$\varphi(\eta) = \varphi_0(\eta) + \sum_{m=0}^{\infty} \varphi_m(\eta) \tag{32}$$

The m^{th}-order deformation problems are:

$$\mathbf{L}_f[f_m(\eta) - \chi_m f_{m-1}(\eta)] = h_f R_m^f(\eta) \tag{33}$$

$$\mathbf{L}_f[\varphi_m(\eta) - \chi_m \varphi_{m-1}(\eta)] = h_\varphi R_m^\varphi(\eta) \tag{34}$$

$$f_m(0) = f_m'(0) = f_m'(\infty) = 0, \qquad \varphi_m(0) = \varphi_m(\infty) = 0 \tag{35}$$

$$\mathbf{R}_f^m(\eta) = (1+K) f_{m-1}'''(\eta) + \sum_{k=0}^{m-1} \left[f_{m-1-k} f_k'' - f_{m-1-k}' f_k' - K\Gamma f_{m-1}'' \sum_{k=0}^{m-1} f_{k-l}'' f_l''' \right] \tag{36}$$

$$R_m^\varphi(\eta) = \varphi_{m-1}''(\eta) - \mathrm{Sc}\ \gamma \varphi_{m-1} + \mathrm{Sc} \sum_{k=0}^{m-1} \left[\varphi_{m-1-k}' f_k - \varphi_k f_{m-1-k}' \right] - \mathrm{Sc}\ \gamma \varphi_{m-1} \tag{37}$$

$$\chi_m = \begin{cases} 0, & m \le 1 \\ 1, & m > 1 \end{cases} \tag{38}$$

The general solutions are:

$$f_m(\eta) = f_m^*(\eta) + C_1 + C_2\ \exp(\eta) + C_3\ \exp(-\eta) \tag{39}$$

$$\varphi_m(\eta) = \varphi_m^*(\eta) + C_4\ \exp(\eta) + C_5\ \exp(-\eta) \tag{40}$$

where f_m^* and φ_m^* are the particular solutions and after invoking eqs. (35) the constants are given by:

$$C_2 = C_4 = 0, \qquad C_3 = \left.\frac{\partial f_m^*(\eta)}{\partial \eta}\right|_{\eta=0}, \qquad C_1 = -C_3 - f_m^*(0), \qquad C_5 = -\varphi_m^*(0) \tag{41}$$

By symbolic software MATHEMATICA, the system of eqs. (33)-(35) can be solved for $m = 1, 2, 3...$

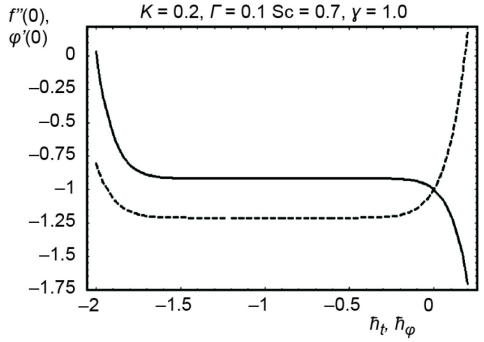

Figure 2. Curves for 15th order of approximations

Table 1. Convergence of the HAM solutions for different order of approximation when $K = 0.2$, $\Gamma = 0.1$, Sc = 0.7, and $\gamma = 0.7$, and numerical values by shooting technique in brackets

Order of approximation	$-f''(0)$	$-\varphi'(0)$
1	0.905000	1.21465
5	0.915895	1.21202
10	0.915896	1.21205
15	0.915896	1.21205
20	0.915896	1.21205
25	0.915896	

Convergence of the HAM solution

The auxiliary parameters, $\hbar_f$ and $\hbar_\varphi$, in the series solutions (31) and (32) play a vital role in adjusting and controlling the convergence. In order to find the admissible values of $\hbar_f$ and $\hbar_\varphi$, the $\hbar_f$ and $\hbar_\varphi$ – curves are plotted for 15th-order of approximations. Figure 2 shows that the range for the admissible values of $\hbar_f$ and $\hbar_\varphi$ are $-1.5 \le \hbar_f \le -0.2$ and $-1.7 \le \hbar_\varphi \le -0.6$. Our computations also indicates that the series given by eqs. (31) and (32) converge in the whole region of η when $\hbar_f = -0.5$ and $\hbar_\varphi = -1$. Table 1 shows the convergence of the homotopy solutions for different order of approximations for $K = 0.2$, $\Gamma = 0.1$, Sc = 0.7, and $\gamma = 1$.

Numerical solution

The numerical solution for eqs. (7)-(9) for different values of non-Newtonian fluid parameters K and Γ, Schimidt number, and chemical reaction parameter subject to the boundary conditions (9) is obtained by the most efficient numerical shooting technique with Runge-Kutta-Fehlberg integration scheme. In this method the coupled non-linear two point boundary value problem is transformed into initial value problem which is a first order system and is obtained by defining new variables. The asymptotic boundary conditions given by eq. (9) were replaced by using a finite value of $\eta_{\max}$ for the similarity variable η as $\eta \to \infty$.

Results and discussion

In this section, the influence of emerging physical parameters on the velocity and concentration fields is studied. Figures 3-8 are prepared to show the variations of K, Γ, Sc, and γ. Figures 3-5 describe the effects of K and Γ on the velocity profile f'. From fig. 3 it can be seen that the velocity field and boundary layer thickness are increasing functions of K. Figure 4 shows that the effect of Γ is opposite to the effect of the material parameter K.

The effects of Sc and γ on the concentration profile are examined in figs. 6-8. The variation of the Schmidt number on φ is shown in fig. 6. The concentration field, φ, decreases when Schmidt number increases. As expected the fluid concentration decreases with an increase in generative chemical reaction parameter ($\gamma > 0$), fig. 7. The fluid concentration, φ, has the opposite behaviour for destructive chemical reaction parameter ($\gamma < 0$) in comparison to the case of generative chemical reaction as shown in fig. 8. To authenticate our present analytical

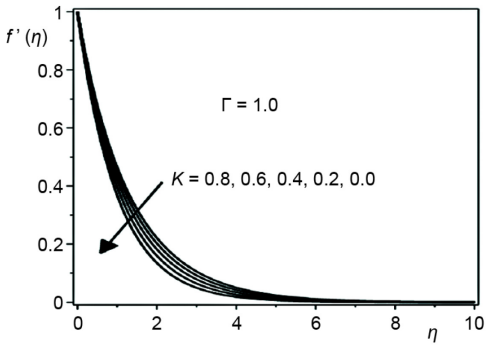

Figure 3. Influence of *K* on *f'*

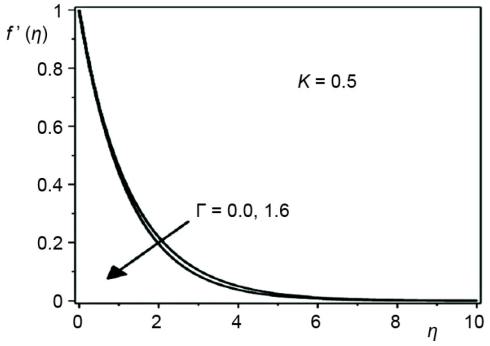

Figure 4. Influence of Γ on *f'*

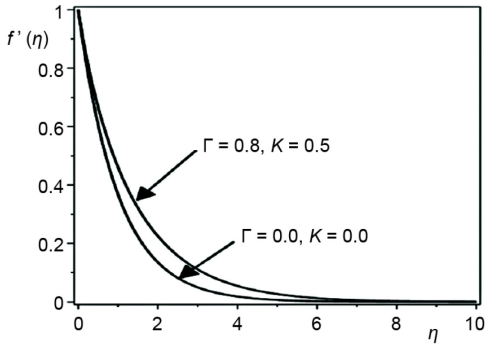

Figure 5. Influence of *K* and Γ on *f'*

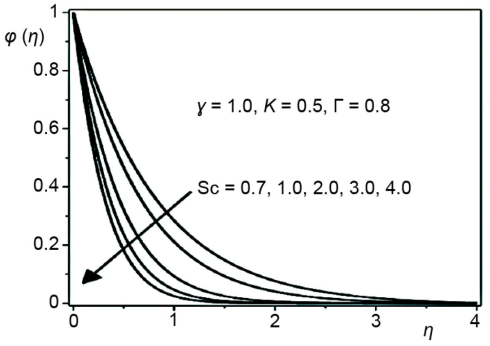

Figure 6. Influence of Sc on *φ*

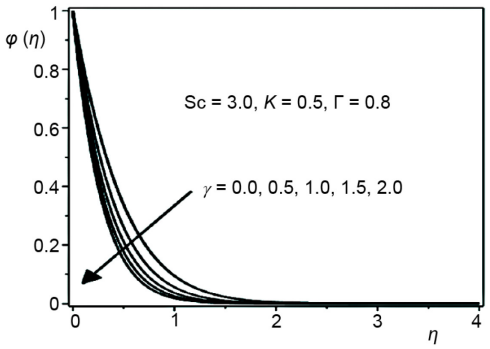

Figure 7. Influence of Sc and *γ* on *φ*

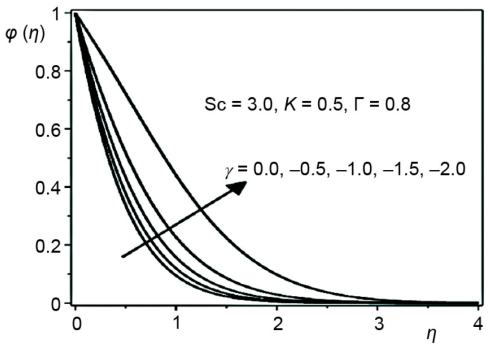

Figure 8. Influence of Sc and *γ* on *φ*

and numerical solutions a comparison is given in tabs. 2 and 3. In these tables numerical values of skin-friction coefficient $\mathrm{Re}_x^{1/2} C_f$ and $f''(0)$ (skin-friction coefficient for viscous fluid *i. e.* $K = \Gamma = 0$) are tabulated. We compared our results obtained by HAM and shooting technique with the results obtained by Javed *et al.* [12] by Keller-box method. All the solutions are found in good harmony. Further, from these tables we observed that the magnitude of $f''(0)$ decreases by increasing K. Similar effects are seen for the skin friction coefficient. It can be seen that the skin friction coefficient is larger for Erying-Powell fluid compare to

Table 2. Comparison of $\mathrm{Re}_x^{1/2} C_f$ and $f''(0)$ for different values of Γ and K

	$\mathrm{Re}_x^{1/2} C_f$			$-f'(0)$		
Γ/K	0.2					
	Present		[12]	Present		[12]
	HAM	Shooting	Keller box	HAM	Shooting	Keller box
0.0	1.0954	1.0952	1.0954	0.9133	0.9131	0.9131
0.1	1.0940	1.0939	1.0940	0.9162	0.9159	0.9159
0.2	1.0924	1.0922	1.0924	0.9193	0.9190	0.9190
0.3	1.0909	1.0909	1.0909	0.9224	0.9222	0.9222
0.4	1.0894	1.0894	1.0894	0.9257	0.9254	0.9254
0.5	1.0878	1.0878	1.0878	0.9289	0.9288	0.9288
0.6	1.0862	1.0862	1.0862	0.9321	0.9322	0.9322
0.7	1.0847	1.0847	1.0847	0.9361	0.9357	0.9357
0.8	1.0829	1.0832	1.0830	0.9398	0.9394	0.9394
0.9	1.0814	1.0816	1.0814	0.9434	0.9431	0.9431
1.0	1.0797	1.0797	1.0798	0.9471	0.9470	0.9470
	1.0					
	HAM	Shooting	Keller box	HAM	Shooting	Keller box
0.0	1.4145	1.4142	1.4142	0.7073	0.7072	0.7071
0.1	1.4108	1.4107	1.4107	0.7116	0.7115	0.7114
0.2	1.4074	1.4072	1.4072	0.7161	0.7159	0.7158
0.3	1.4039	1.4036	1.4036	0.7205	0.7206	0.7205
0.4	1.3999	1.3999	1.3999	0.7254	0.7255	0.7254
0.5	1.3965	1.3961	1.3961	0.7305	0.7306	0.7305
0.6	1.3925	1.3922	1.3922	0.7360	0.7362	0.7360
0.7	1.3887	1.3883	1.3883	0.7148	0.7419	0.7418
0.8	1.3843	1.3842	1.3842	0.7479	0.7480	0.7479
0.9	1.3802	1.3801	1.3801	0.7544	0.7546	0.7544
1.0	1.3761	1.3758	1.3758	0.7615	0.7616	0.7615

viscous fluid. The values of the surface mass transfer, $-\varphi'(0)$, are presented in tab. 3. Table 3 depicts that the surface mass transfer, $-\varphi'(0)$, increases by increasing K and Γ. The surface mass transfer, $-\varphi'(0)$, increases by increasing both Schmidt number and γ. Also an excellent agreement is found between homotopy analysis and shooting method.

Table 3. Comparison of $-\varphi'(0)$ for different values of Γ, K, Sc, and γ

Γ	K	Sc	γ	$-\varphi'(0)$	
				HAM	Shooting
0.1	0.2	1	1	1.4696	1.4696
0.3				1.4692	1.4692
0.5				1.4687	1.4687
0.5	0.5			1.4799	1.4799
	1			1.4938	1.4937
0.1	0.2	0.2	1	1.6074	1.6073
		0.6		1.1145	1.1145
		0.8		1.3030	1.3030
0.1	0.2	1	1	1.4696	1.4696
			1.5	1.6395	1.6395
			1.8	1.7324	1.7324

Conclusions

The present study describes the flow of an Erying-Powell fluid with mass transfer effect. Analytical and numerical solutions to the governing non-linear problem are presented. Analysis of tab. 1 shows that solution up to 10^{th} order of approximations is enough. Comparison of the present study with [12] is shown in a limiting sense. It is observed that velocity field and boundary layer thickness are increasing functions of Erying fluid parameter, K. Further, the mass transfer rate is larger in Erying Powell fluid as compared to Newtonian viscous fluid.

Nomenclature

b – positive constant, [molkg^{-1}m^{-1}]
c – stretching rate, [s^{-1}]
C – concentration field, [molkg^{-1}]
C_w – concentration at wall, [molkg^{-1}]
C_{fx} – skin friction coefficient, [–]
D – mass diffusion, [m^{2}s^{-2}]
f – dimensionless stream function, [–]
K – fluid parameter $(= 1/\mu\tilde{\beta}C^*)$
Re_x – local Reynold number
Sc – Schmidt number $(= \nu/D)$
Sh – Sherwood number
u, v – velocity components, [ms^{-1}]
U_w – velocity at wall, [ms^{-1}]
x, y – space co-ordinates, [m]

Greek symbols

γ – chemical reaction parameter $(= K_1/c)$
η – dimensionless space variable, [–]
ν – kinematic viscosity, [m^{2}s^{-1}]
ρ – fluid density, [kgm^{-3}]
τ – surface shear stress, [kgm^{-3}s^{-2}]
φ – dimensionless concentration, [–]

Reference

[1] Ishak, A., *et al.*, Heat Transfer over a Stretching Surface with Variable Heat Flux in Micropolar Fluids, *Phys Lett A, 372* (2008), 5, pp. 559-561
[2] Fetecau, C., *et al.*, On the Oscillating Motion of an Oldroyd-B Fluid Between Two Infinite Circular Cylinders, *Comput Math Appl, 59* (2010), 8, pp. 2836-2845
[3] Fetecau, C., *et al.*, A Note on the Second Problem of Stokes for Maxwell Fluids, *Int. J. Non-Linear Mech., 44* (2009), 10, pp. 1085-1090
[4] Fetecau, C., *et al.*, On the First Problem of Stokes for Burgers' Fluid, I: *Non-linear Anal.: Real World Appl., 10* (2009), 4, pp. 2183-2194
[5] Vieru, D., Rauf, A., Stokes Flows of a Maxwell Fluid with Wall Slip Condition, *Can. J. Phys., 89* (2011), 10, pp. 1061-1071
[6] Vieru, D., Zafar, A. A., Some Couette Flows of a Maxwell Fluid with Wall Slip Condition, *Appl. Math. Inf. Sci., 7* (2013), 1, pp. 209-219

[7] Imran, M. A., *et al.*, Exact Solutions for Oscillating Motion of a Second Grade Fluid along an Edge with Mixed Boundary Conditions, *Chem. Eng. Comm., 199* (2012), 9, pp. 1085-1101
[8] Qasim, M., Heat and Mass Transfer in a Jeffrey Fluid over a Stretching Sheet with Heat Source/Sink, *Alexandria Engineering Journal*, *52* (2013), 4, pp. 571-575
[9] Khan, I., *et al.*, Stokes' Second Problem for Magnetohydrodynamics Flow in a Burgers' Fluid: Cases $\gamma = \lambda^2/4$ and $\gamma > \lambda^2/4$, *PLoS ONE, 8* (2013), 5, e61531
[10] Qasim, M., *et al.*, Heat Transfer in a Micropolar Fluid over a Stretching Sheet with Newtonian Heating, *PLoS ONE, 8* (2013), 4, e59393
[11] Powell, R. E., Eyring, H., Mechanisms for the Relaxation Theory of Viscosity, *Nature, 154* (1944), 3909, pp. 427-428
[12] Javed, T., *et al.*, Flow of an Eyring-Powell Non-Newtonian Fluid over a Stretching Sheet, *Chem. Eng. Comm., 200* (2013), 3, pp. 327-336
[13] Hayat, T., *et al.*, Flow of an Eyring-Powell Fluid with Convective Boundary Conditions, *J. Mech., 29* (2009), 2, pp. 217-224
[14] Patel, M., Timol, M. G., Numerical Treatment of Powell-Eyring Fluid Flow Using Method of Satisfaction of Asymptotic Boundary Conditions (MSABC), *Appl. Num. Math., 59* (2009), 10, pp. 2584-2592
[15] Eldabe, N. T. M., *et al.*, Effect of Couple Stresses on the MHD of a Non-Newtonian Unsteady Flow between Two Parallel Porous Plates, *Z. Naturforsch*. *58* (2003), 4, pp. 204-210
[16] Crane, L. J., Flow Past a Stretching Plate, *Z. Angew. Math. Mech., 21* (1970), 4, pp. 645-647
[17] Andersson, H. I., *et al.* Diffusion of Chemically Reactive Species from a Stretching Sheet, *Int. J. Heat Mass Transfer, 37* (1994), 4, pp, 659-664
[18] Takhar, H. S., *et al.*, Flow and Mass Transfer on a Stretching Sheet with Magnetic Field and Chemical Reactive Species, *Int. J. Eng. Sci., 38* (2000), 12, pp. 1303-1314
[19] Akyildiz, F. T., *et al.*, Diffusion of Chemical Reactive Species in Porous Medium over a Stretching Sheet, *J. Math. Anal. Appl., 320* (2006), 1, pp. 322-339
[20] Hayat, T., *et al.*, MHD Flow and Mass Transfer of Upper-Convected Maxwell Fluid past a Porous Shrinking Sheet with Chemical Reaction Species, *Phys. Lett. A 372* (2008), 26, pp. 4698-4704
[21] Liao, S. J., *Beyond Perturbation: Introduction to Homotopy Analysis Method*, Chapman and Hall, CRC Press, Boca Raton, Fla., USA, 2003
[22] Liao, S. J., *Homotopy Analysis Method in Non-Linear Differential Equations*, Springer, New York, USA, 2011
[23] Butt, A. S., Ali, A., A Computational Study of Entropy Generation in Magnetohydrodynamic Flow and Heat Transfer over an Unsteady Stretching Permeable Sheet, *The European Physical Journal Plus.,* 129 (2014), 1, pp. 1-13
[24] Qasim, M., *et al*., MHD Boundary Layer Slip Flow and Heat Transfer of Ferrofluid along a Stretching Cylinder with Prescribed Heat Flux, *Plos One*, *9* (2014), 1, e83930
[25] Mabood, F., Khan, W. A., Homotopy Analysis Method for Boundary Layer Flow and Heat Transfer over a Permeable Flat Plate in a Darcian Porous Medium with Radiation Effects, *Journal of the Taiwan Institute of Chemical Engineers, 45* (2014), 4, pp. 1217-1224
[26] Nadeem, S., *et al.*, Heat Transfer Analysis of Water-Based Nanofluid over an Exponentially Stretching Sheet, *Alexandria Engineering Journal*, *53* (2014), 1, pp. 219-224

Paper submitted: November 29, 2013
Paper revised: July 15, 2014
Paper accepted: July 27, 2014